Letter

Polymer Nanocomposite Microactuators for On-Demand Chemical Release via High-Frequency Magnetic Field Excitation

Seyed M. Mirvakili,* Quynh P. Ngo, and Robert Langer*

Cite This: *Nano Lett.* 2020, 20, 4816−4822

Read Online

ACCESS | Metrics & More | Article Recommendations | Supporting Information

ABSTRACT: On-demand delivery of substances has been demonstrated for various applications in the fields of chemistry and biomedical engineering. Single-pulse release profile has been shown previously for micro/nanoparticles in different form factors. However, to obtain a sustained release, a pulsatile release profile is needed. Here, we demonstrate such a release profile from polymer magnetic nanocomposite microspheres loaded with chemicals. By exciting the microactuators with AC magnetic fields, we could achieve up to 61% cumulative release over a five-day period. One of the main advantages of using a magnetic stimulus is that the properties of the environment (e.g., transparency, density, and depth) in which the particles are located do not affect the performance. The operating magnitude of the magnetic field used in this work is safe and does not interact with any nonmetallic materials. The proposed approach can potentially be used in microchemistry, drug delivery, lab-on-chip, and microrobots for drug delivery.

KEYWORDS: *pulsatile release, wireless excitation, on-demand delivery, magnetic nanoparticles, microactuators*
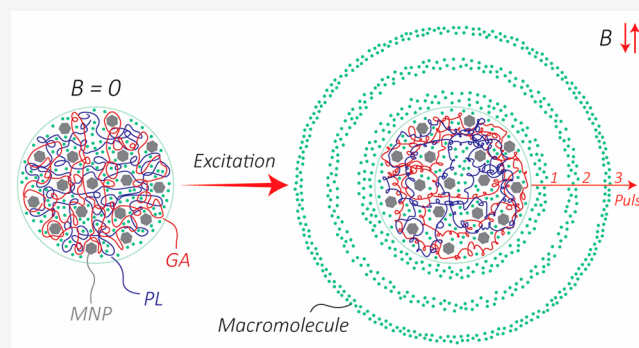
INTRODUCTION

Triggering chemical carriers by relying on the intrinsic physical or chemical properties of the target environment (e.g., pH, concentration gradient, enzymes) are explored extensively for controlled delivery of chemicals for various applications. However, to have better control of the dosage, time, and location of the release in heterogeneous environments, triggering the release mechanism by an external energy source is vital. Such systems are employed in lab-on-a-chip devices, polymeric microspheres/cubes, and microcapsules to enable spatial and temporal control of chemical reactions. Depending on the nature of the release environment, different stimuli can be employed. Some of the state-of-the-art techniques include light-triggered (e.g., high-power infrared laser) microcarriers,[1−6] wireless microchips,[7,8] shape-memory materials,[9−11] stimuli-responsive hydrogels,[12,13] ultrasound-triggered carriers,[14−17] and electric-field responsive conducting polymers.[18−20] However, almost all of the mentioned techniques need direct contact with an energy source (e.g., laser or light), can interact with the release environment (e.g., electric field, light), or can be detrimental to the environment during the excitation (e.g., ultrasound).

In the present work, we are proposing a method of fabrication for spherical microactuators that can release a preloaded chemical when excited with AC magnetic fields. The microactuators are made of magnetic nanoparticles blended with a biodegradable polymer. The magnetic nanoparticles in the microspheres undergo inductive heating when an AC magnetic field is applied. As a result, the temperature of the microsphere increases and expands the free space inside the network. This expansion escalates the release rate from the particles during the excitation periods.

One of the main advantages of using a magnetic stimulus is that it has minimal interaction with the release environment. Moreover, the physical properties of the environment (e.g., transparency, mass density, and depth) in which the particles are located do not affect the performance. Additionally, the DC magnetic field can be utilized to guide the particles to the site of action prior to excitation with an AC magnetic field. This AC/DC combination of excitation allows precise control over the spatial and temporal release of the chemicals.

Heat generation with AC magnetic field, such as in induction heating, is extensively used in different applications—from cooking appliances and metal engineering to DNA engineering,[21] cancer cells eradication via hyperthermia,[22,23] and drug delivery.[24−26] In drug delivery, inductive heating of micro/nanoparticles employed in drug carriers is used to
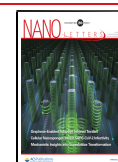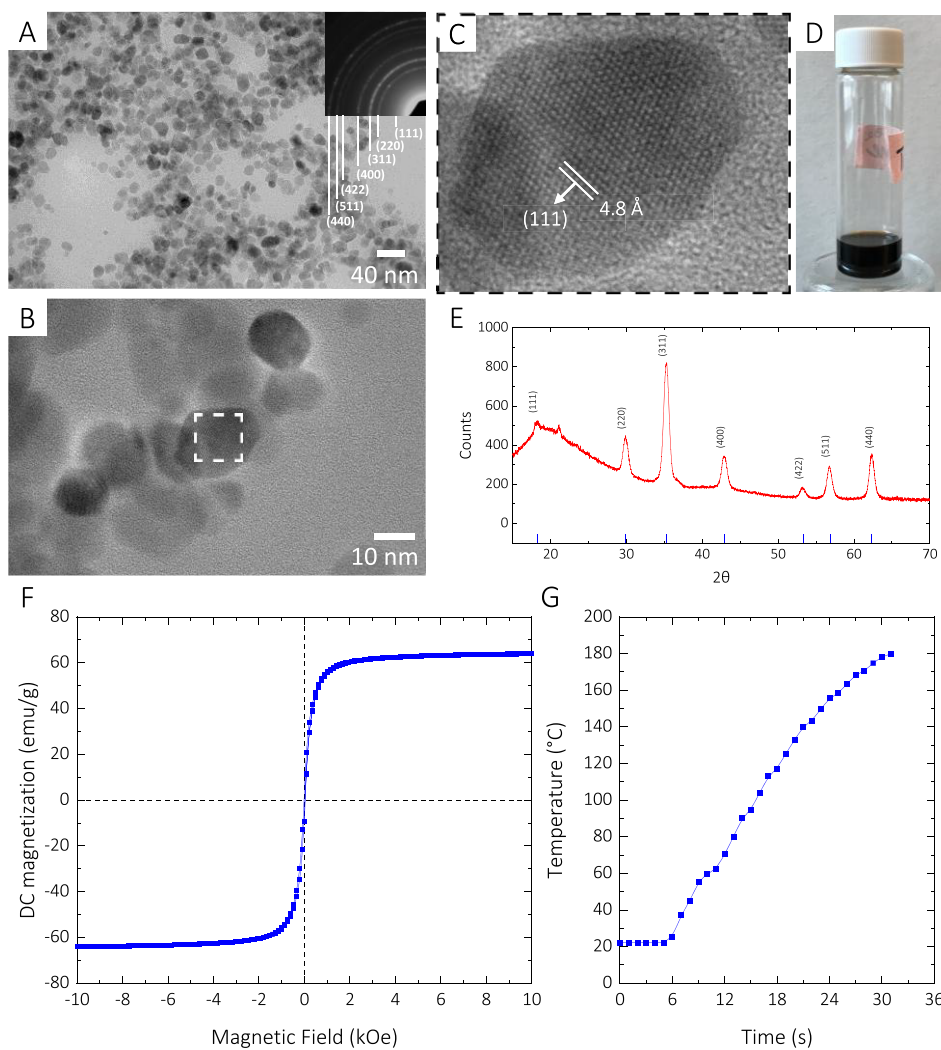
Figure 1. (A) TEM image of the synthesized Mg-γFe$_2$O$_3$ MNPs. (B,C) High-resolution TEM image of the Mg-γFe$_2$O$_3$ MNPs. (D) Mg-γFe$_2$O$_3$ MNPs dispersed in toluene. (E) X-ray diffraction analysis suggesting that the MNPs are Mg-γFe$_2$O$_3$. (F) DC major hysteresis loops of the Mg-γFe$_2$O$_3$ MNPs. (G) Inductive heating characteristics of the Mg-γFe$_2$O$_3$ MNPs.

provide controllability over the release profile. For example, it is demonstrated that mesoporous silica nanoparticles coated with drug-loaded azo-functionalized PEG and Fe$_3$O$_4$ MNPs can release the drug when excited with an AC magnetic field.[27] Similarly, it is shown that nanocapsules made of porous silica shell can be loaded with Fe$_3$O$_4$ and drugs for delivery in tumors.[28] Thermoresponsive polymers and hydrogels such as poly-N-isopropylacrylamide (pNIPAM) exhibit reversible volume phase transition in response to temperature change.[29] When doped with magnetic nanoparticles, they can be either loaded with a drug or used as a valve to open/close drug cages to provide a pulsatile release profile.[30−33] Biodegradable polymers in the form of core−shell (drug in the core, MNPs in the shell) or nanoparticles have been demonstrated with a single-pulse release profile.[34−36] While a single-pulse release profile is useful for one-time chemical delivery, for a sustained release a pulsatile-release profile is essential. In this work, we are employing poly(lactic-co-glycolic acid) microspheres loaded with magnetic nanoparticles to obtain such a release profile when excited with AC magnetic fields.

PLGA is a biodegradable polymer and is often used in drug delivery and degradable electronics.[25,37] Here, we demonstrate

that the microsphere particles with an average diameter of 15 μm can release the fluorescent model compound when inductively heated. We achieved up to 61% cumulative release upon multiple excitations over a five-day period.

Our investigations show that the release mechanism is primarily due to an increase in the diffusion rate, which is due to the expansion of the free space in the polymer network. Therefore, we can categorize these microparticles as microactuators.[29] These microactuators act as a molecular switch that controls the diffusion rate of the infiltrated macromolecules.

■ RESULTS AND DISCUSSION

Magnetic Nanoparticles. Metallic and, more specifically, magnetic particles generate heat when exposed to an alternating magnetic field. The heating mechanism for metallic particles is primarily due to the formation of an eddy current, which leads to Joule heating. For magnetic nanoparticles, depending on their size the heating mechanism is a combination of hysteresis losses (for multimagnetic domains) and Néel-Brownian relaxation (for single domain particles such as superparamagnetic nanoparticles).[38,39] As the energy
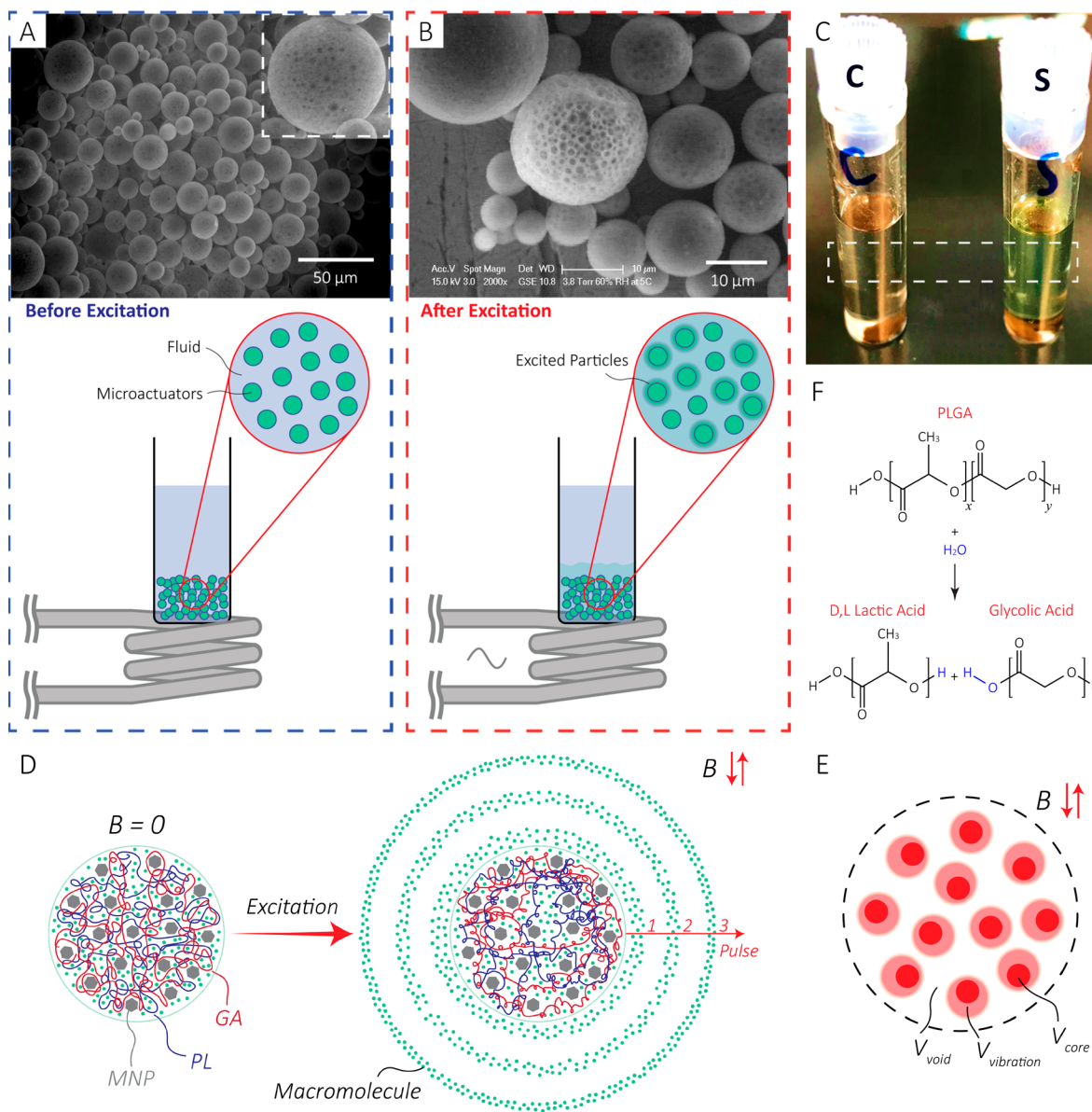
Figure 2. (A) Before excitation: Scanning electron microscope image of the particles before excitation with the setup. Inset: A zoomed-in image of a 50 μm microactuator shows the MNPs agglomerated in the structure. (B) After excitation: Higher magnification scanning electron microscope image. As shown in the illustration, the sample vial was held over the coil to minimize any potential heat transfer. For better visual illustration, only a group of green spheres are illustarted releasing. (C) Optical image of the control (left) and sample (right) after excitation of a solution (13.5 g/L) with 1.8 kW excitation power for 20 min. As shown by the image, the sample solution's color is greener than that of the control solution. (D) Illustration of the release mechanism. When excited, the temperature of the polymer increases, which leads to an increase in the mobility of the polymer chains. Therefore, the free volume inside the network increases, enabling a higher diffusion rate of the macromolecules. For the purpose of illustration, PL and GA are shown in distinct colors with a 50:50 length ratio. In reality, the polymer is a long chain with the PL and GA distributed along the length as shown in Figure 2F. (E) The free volume inside the network comprises the void volume (V_{void}), and the vibration volume ($V_{\text{vibration}}$) formed due to the mobility of the polymer chains. V_{core} denotes the core/occupied volume. (F) The hydrolysis reaction for PLGA producing D,L lactic acid and glycolic acid.

converting units, magnetic nanoparticles that can generate more heat under excitation with smaller alternating magnetic field amplitudes are more advantageous. In other words, the higher the magnetization value is, the more efficient they are in converting heating at a specified alternating magnetic field.

Here, we used iron oxide (Fe_3O_4 or γ-Fe_2O_3) as the base material for our magnetic nanoparticles and doped it with Mg (magnesium). The product, Mg-γFe_2O_3, exhibits better magnetization properties than Fe_3O_4. Moreover, it is biocompatible/degradable and suitable for biomedical applications.[40] Through a thermal decomposition method, we

synthesized the Mg-γFe_2O_3 MNPs with the diameters ranging from 12 to 15 nm (Experimental Section) (Figure 1A−D). Our X-ray powder diffraction (XRD) analysis confirms that the compound composition is Mg-γFe_2O_3 (Figure 1E). The synthesized Mg-γFe_2O_3 MNPs exhibit DC magnetization of around 62 emu/g (Figure 1F), which is higher than that of the pristine Fe_3O_4 MNPs.[41] To measure the amount of heat the substance can generate, we excited 197 mg of the Mg-γFe_2O_3 at an input power of 900 W. The MNPs could raise the temperature from 20 to 190 °C in less than 25 s (Figure 1G).
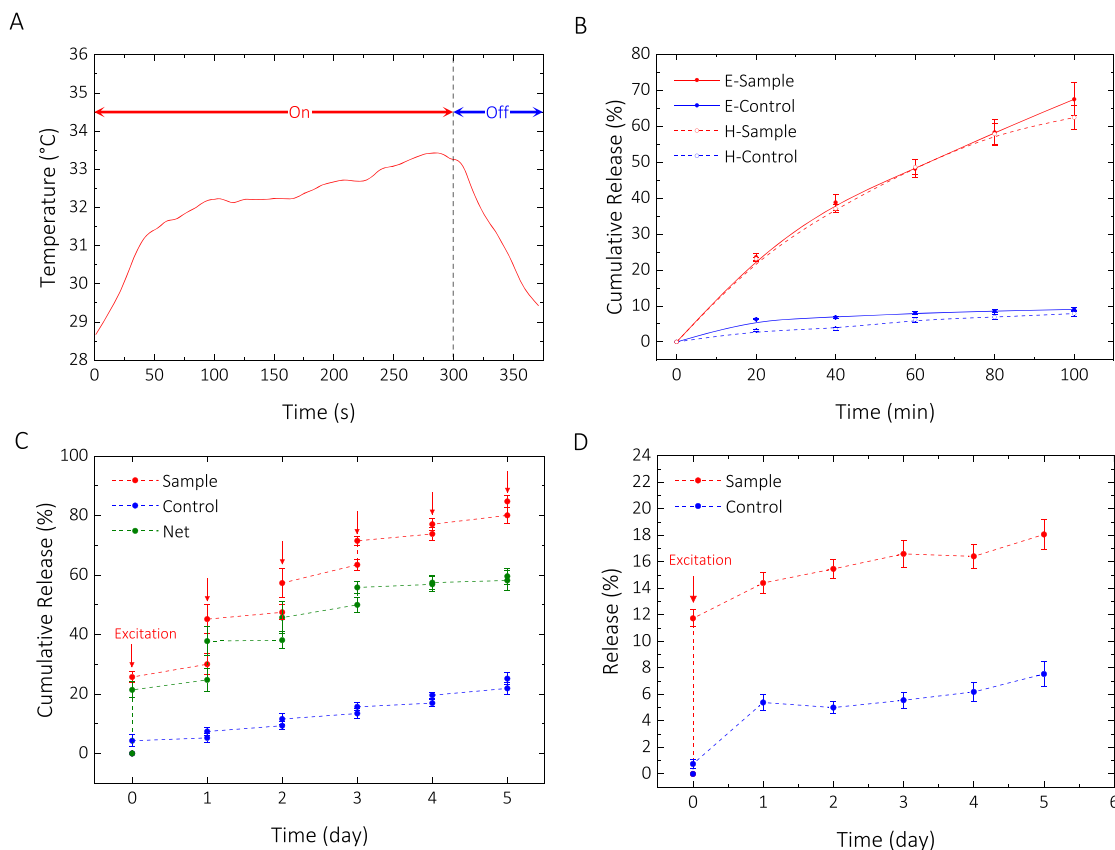
Figure 3. (A) Temperature profile for a sample with a microparticle concentration of 13.5 g/L in DI water excited for 5 min at an input power of 1.8 kW. (B) Cumulative release with inductive excitation (E-Sample/Control) and temperature-controlled hot plate (H-Sample/Control). (C) Sample: Cumulative percentage of initial loading released upon inductive excitation. Control: Cumulative percentage of initial loading released passively. The jumps occur while the control was at room temperature. The net release (i.e., $CR_{sample} - CR_{control}$) shows a net cumulative release of 61% over a five-day excitation period. (D) Excitation at 1.8 kW and monitoring for 5 days. The profile consists of an initial pulse (active release) followed with a slow and sustained release (passive release) over time.

Polymer Microparticles. PLGA-based micro/nanoparticles have been studied for application in the controlled-release of drugs and chemicals.[35,36,42] By controlling the LA/GA ratio and molecular weight, polymer properties such as the glass transition temperature can be modified to control the release profile.[42] One key property of polymers like PLGA is that by increasing their temperature close to the glass transition temperature, diffusion rate of the trapped macromolecules inside of their network increases. In this work, we are utilizing this property to control the release rate for each excitation.

To fabricate the microactuators, the resulting Mg-γFe$_2$O$_3$ MNPs were mixed with the PLGA precursor and used in a double emulsion process to encapsulate the fluorescent model compound (Experimental Section). This technique yielded microparticles, mostly ranging from 10 to 15 μm in diameter (Supporting Information). The scanning electron microscope image of the particles shows some degree of MNP aggregation in the microspheres (black spots shown in Figure 2A inset), which can be explained by the fact that the dispersion of MNPs and PLGA is energetically unfavorable. As a result, the MNPs aggregated and formed a separate phase from PLGA. Upon inductively exciting the microactuators (Figure 2B, Experimental Section), the MNPs increase the temperature of the microactuators locally and rapidly, which escalates the release rate. For prolonged excitations, the temperature of the solution increases until a thermal equilibrium is reach with the surrounding environment. Figure 2C visually demonstrates the excitation/release results. In this experiment, the two samples were identically prepared; the control sample (C) did not undergo excitation while the sample (S) was excited at an input power of 1.8 kW. The increase in the release rate can be explained by the fact that when the temperature approaches the T_g, mobility of the polymer chains increases. This increase in mobility expands the free space inside the network, which translates to an increase in the diffusion rate (Figure 2D,E).[43,44] In longer time scales, the degradation mechanism for PLGA in an aqueous environment is mainly through a hydrolysis process (also temperature dependent) which produces D,L lactic acid and glycolic acid (Figure 2F).[37,45,46]

To examine the contribution of the generated heat from MNPs to the overall temperature of the sample/solution, we measured the temperature as a function of time with a fiber optic temperature sensor (Experimental Section). As shown in Figure 3A, the overall temperature of the solution increases but does not reach a steady state during the excitation period. Because of the heat transfer to the environment, we spectulate the local temperature of the MNP-aggregates is higher than the solution temperature for the excitation periods that we chose.

To further examine if the increase in temperature provides the dominant contribution to the release mechanism, we designed a controlled experiment. We ramped the temperature

of the solution (13.5 g/L) to 37 °C homogeneously with a hot plate and monitored the release every 20 min. In parallel, we excited an identically prepared sample inductively at an input power of 1.8 kW and monitored the solution every 20 min. The control samples for both experiments were kept at room temperature during the entire experiment. As Figure 3B illustrates, as expected, both techniques resulted in a very similar release profile over time.

To show the release efficacy of the microparticles, we excited a sample for 20 min at an input power of 1.8 kW every 24 h while the control sample was kept at room temperature during the excitation experiment. Both samples were stored at 4 °C between the excitation intervals. We observed a multiple-pulse release profile over 5 days. Figure 3C shows the cumulative release of the fluorescent model compound, sodium fluorescein, upon excitation (sample), and passively over time (control). As shown on the plot, the control sample passively released 2.5−3% at room temperature, while the sample released up to 24% during the excitation period. Overall cumulative release of 61% was achieved over 5 days via inductive excitation. To investigate the potential effect of the first excitation on the passive release rate, we prepared two identical samples, one was excited at 1.8 kW input power, while the other one was kept as the control at room temperature during the excitation. Both samples were stored at 4 °C for the entire waiting period. As illustrated in Figure 3D, the passive release profiles of the control and the excited sample are very similar. This further justifies our rationale for categorizing the microparticles as microactuators.

Future Work. The magnetic flux density (i.e., B) scales with inverse of the coil diameter (Supporting Information). Moreover, the effective heating power per mass of the magnetic particles due to hysteresis losses scales linearly with the frequency ($\propto f$).[39] Therefore, we can scale down the coil (e.g., planar microcoils[47]) and excite it with a much higher range of frequencies (GHz as opposed to kHz) with an RF power amplifier. This miniaturization allows for having small devices that can be used for on-demand drug delivery for diseases and conditions with symptoms occurring at irregular and unpredictable time intervals (e.g., psychogenic pain, psychotic disorders, blood coagulation).

To further enhance the efficacy and efficiency of the design, the magnetic nanoparticles can be engineered to have higher DC magnetization. This modification of magnetic properties can lead to higher rate of heat generation per mass of the nanoparticles for a specified excitation power.

CONCLUSION

In this work, we proposed a fabrication technique for making microactuators made of PLGA infiltrated with MNPs and demonstrated that the particles could be used for on-demand chemical delivery with pulsatile release profile. We measured a net cumulative mass release of up to 61% for a sample excited for 20 min at an input power of 1.8 kW in 24 h intervals every day for 5 days. Moreover, we showed that the technique could be used as a single-pulse release system as well. The spatial and temporal controllability of our proposed technique enables application in microfluidic chips, lab-on-chip, microreactors, drug delivery, cell engineering, and micro/nanoliter chemical systems in general.

EXPERIMENTAL SECTION

Magnetic Particle Preparation. The Mg-γFe$_2$O$_3$ MNPs were prepared by following a common procedure for synthesizing iron-based MNPs but with some minor modifications.[48] First, we mixed 1.2 mmol of oleic acid (≥99%, Sigma-Aldrich) with 20 mL of benzyl ether. Then, 0.13 mmol of magnesium acetate tetrahydrate (≥98%, Sigma-Aldrich) and 2 mmol of iron(III) acetylacetonate (97%, Sigma-Aldrich) were added to the solution and magnetically stirred for 10 min in a 50 mL round-bottom flask. The solution was bubbled with Ar/O$_2$ (20% oxygen balance argon Size 80) at a flow rate of 100 mL/min and heated up to 200 °C and kept at that temperature for 50 min under a fume hood. The solution was then heated up to 296 °C and kept at that temperature for 60 min. The flask was then removed and cooled down at room temperature. Toluene was added to the flask and placed on a vortex mixer for 5 min. The procedure was repeated until the entire substance was dispersed in toluene and was transferred to multiple 40 mL scintillation vials. A rotary evaporator was used to remove the toluene from the solution.

Microparticle Preparation. Microparticles were prepared using a water-in-oil-in-water (w$_1$/o/w$_2$) double emulsion method. We chose this technique because it allows encapsulating water-soluble molecules inside each particle (i.e., sodium fluorescein in this study). The first water phase (w$_1$) consists of the sodium fluorescein (F6377, Sigma-Aldrich) dissolved in water at a concentration of 5 g/L. The oil phase (o) was prepared by dispersing 62.5 mg of MNPs in 1 mL of DCM by sonication and adding 200 mg of 502H PLGA 5050 (Evonik, Germany). In parallel, 50 mL of 1 wt % PVA in water was prepared as the second water phase (w$_2$). All fabrication steps were done with a tip sonicator, while the temperature of the phases was kept low with an ice bath. Two hundred microliters of w$_1$ was added to o and homogenized for 20 s at a 35% amplitude. This first emulsion was then immediately added to w$_2$ and homogenized for 1 min. The final emulsion was stirred for 3 h at 250 rpm to evaporate DCM completely. The resulting particles were washed four times by centrifugation at 3200×g for 5 min, decanted, and washed with water. They were stored at 4 °C for further experimentation. We estimate the mass concentration of the MNPs in the PLGA microsphere to be 23.8%.

Excitation/Measurement Techniques and Equipment. For excitation, we used a 3 kW induction heater (Precision Power Systems & Technology, model number 3-135/400-2) with controllable output power. The induction coil was custom-made to match the diameter of the glass vials (i.e., 17.5 mm) (Supporting Information). The coil was cooled down by circulating cold water from a bucket filled continuously with ice and water. To investigate any heat transfer from the induction coil to the solution in the glass vial, we excited a glass vial filled with water at 1.8 kW for 30 min. We observed less than 2 °C change in the temperature of the water. The resonance frequency of the LC tank made with our custom-made coil was around 220 kHz throughout the experiments.

We use a plate reader (Tecan, Infinite 200) to measure the amount of sodium fluorescein released during the experiments. The calibration procedure and curve are included in the Supporting Information. All of the excitation/release experiments in this work are reproduced at least three times.

ASSOCIATED CONTENT

Supporting Information

The Supporting Information is available free of charge at https://pubs.acs.org/doi/10.1021/acs.nanolett.0c00648.

Detailed experimental procedures (PDF)

AUTHOR INFORMATION

Corresponding Authors

Seyed M. Mirvakili − *Koch Institute for Integrative Cancer Research, Massachusetts Institute of Technology, Cambridge, Massachusetts 02139, United States;* orcid.org/0000-0002-8062-6833; Email: seyed@mit.edu

Robert Langer − *Koch Institute for Integrative Cancer Research, Massachusetts Institute of Technology, Cambridge, Massachusetts 02139, United States;* orcid.org/0000-0003-4255-0492; Email: rlanger@mit.edu

Author

Quynh P. Ngo − *Department of Materials Science and Engineering, Massachusetts Institute of Technology, Cambridge, Massachusetts 02139, United States*

Complete contact information is available at:
https://pubs.acs.org/10.1021/acs.nanolett.0c00648

Notes

The authors declare no competing financial interest.

ACKNOWLEDGMENTS

REFERENCES

(1) Yavuz, M. S.; Cheng, Y.; Chen, J.; Cobley, C. M.; Zhang, Q.; Rycenga, M.; Xie, J.; Kim, C.; Song, K. H.; Schwartz, A. G.; Wang, L. V.; Xia, Y. Gold Nanocages Covered by Smart Polymers for Controlled Release with Near-Infrared Light. *Nat. Mater.* **2009**, *8* (12), 935−939.

(2) Lin, Q.; Huang, Q.; Li, C.; Bao, C.; Liu, Z.; Li, F.; Zhu, L. Anticancer Drug Release from a Mesoporous Silica Based Nano-photocage Regulated by Either a One- or Two-Photon Process. *J. Am. Chem. Soc.* **2010**, *132* (31), 10645−10647.

(3) Rwei, A. Y.; Lee, J.-J.; Zhan, C.; Liu, Q.; Ok, M. T.; Shankarappa, S. A.; Langer, R.; Kohane, D. S. Repeatable and Adjustable On-Demand Sciatic Nerve Block with Phototriggerable Liposomes. *Proc. Natl. Acad. Sci. U. S. A.* **2015**, *112* (51), 15719−15724.

(4) Tong, R.; Chiang, H. H.; Kohane, D. S. Photoswitchable Nanoparticles for in Vivo Cancer Chemotherapy. *Proc. Natl. Acad. Sci. U. S. A.* **2013**, *110* (47), 19048−19053.

(5) Zhan, C.; Wang, W.; McAlvin, J. B.; Guo, S.; Timko, B. P.; Santamaria, C.; Kohane, D. S. Phototriggered Local Anesthesia. *Nano Lett.* **2016**, *16* (1), 177−181.

(6) Wang, W.; Liu, Q.; Zhan, C.; Barhoumi, A.; Yang, T.; Wylie, R. G.; Armstrong, P. A.; Kohane, D. S. Efficient Triplet−Triplet Annihilation-Based Upconversion for Nanoparticle Phototargeting. *Nano Lett.* **2015**, *15* (10), 6332−6338.

(7) Santini, J. T.; Cima, M. J.; Langer, R. A Controlled-Release Microchip. *Nature* **1999**, *397* (6717), 335−338.

(8) Farra, R.; Sheppard, N. F.; McCabe, L.; Neer, R. M.; Anderson, J. M.; Santini, J. T.; Cima, M. J.; Langer, R. First-in-Human Testing of a Wirelessly Controlled Drug Delivery Microchip. *Sci. Transl. Med.* **2012**, *4*, 122ra21−122ra21.

(9) Lendlein, A.; Jiang, H.; Jünger, O.; Langer, R. Light-Induced Shape-Memory Polymers. *Nature* **2005**, *434* (7035), 879−882.

(10) Balk, M.; Behl, M.; Wischke, C.; Zotzmann, J.; Lendlein, A. Recent Advances in Degradable Lactide-Based Shape-Memory Polymers. *Adv. Drug Delivery Rev.* **2016**, *107*, 136−152.

(11) Mirvakili, S. M.; Hunter, I. W. A Torsional Artificial Muscle from Twisted Nitinol Microwire; *Proc. SPIE*, **2017**; Vol. *10163*, pp 101630S−101630S-7. .

(12) Fong, J.; Xiao, Z.; Takahata, K. Wireless Implantable Chip with Integrated Nitinol-Based Pump for Radio-Controlled Local Drug Delivery. *Lab Chip* **2015**, *15* (4), 1050−1058.

(13) Rahimi, S.; Sarraf, E. H.; Wong, G. K.; Takahata, K. Implantable Drug Delivery Device Using Frequency-Controlled Wireless Hydrogel Microvalves. *Biomed. Microdevices* **2011**, *13* (2), 267−277.

(14) Yan, F.; Li, L.; Deng, Z.; Jin, Q.; Chen, J.; Yang, W.; Yeh, C.-K.; Wu, J.; Shandas, R.; Liu, X.; Zheng, H. Paclitaxel-Liposome−Microbubble Complexes as Ultrasound-Triggered Therapeutic Drug Delivery Carriers. *J. Controlled Release* **2013**, *166* (3), 246−255.

(15) Wang, C.-H.; Kang, S.-T.; Lee, Y.-H.; Luo, Y.-L.; Huang, Y.-F.; Yeh, C.-K. Aptamer-Conjugated and Drug-Loaded Acoustic Droplets for Ultrasound Theranosis. *Biomaterials* **2012**, *33* (6), 1939−1947.

(16) Krasovitski, B.; Frenkel, V.; Shoham, S.; Kimmel, E. Intramembrane Cavitation as a Unifying Mechanism for Ultrasound-Induced Bioeffects. *Proc. Natl. Acad. Sci. U. S. A.* **2011**, *108*, 3258.

(17) Dromi, S.; Frenkel, V.; Luk, A.; Traughber, B.; Angstadt, M.; Bur, M.; Poff, J.; Xie, J.; Libutti, S. K.; Li, K. C. P.; Wood, B. J. Pulsed-High Intensity Focused Ultrasound and Low Temperature−Sensitive Liposomes for Enhanced Targeted Drug Delivery and Antitumor Effect. *Clin. Cancer Res.* **2007**, *13* (9), 2722−2727.

(18) Ge, J.; Neofytou, E.; Cahill, T. J.; Beygui, R. E.; Zare, R. N. Drug Release from Electric-Field-Responsive Nanoparticles. *ACS Nano* **2012**, *6* (1), 227−233.

(19) Kagatani, S.; Shinoda, T.; Konno, Y.; Fukui, M.; Ohmura, T.; Osada, Y. Electroresponsive Pulsatile Depot Delivery of Insulin from Poly(Dimethylaminopropylacrylamide) Gel in Rats. *J. Pharm. Sci.* **1997**, *86* (11), 1273−1277.

(20) George, P. M.; LaVan, D. A.; Burdick, J. A.; Chen, C.-Y.; Liang, E.; Langer, R. Electrically Controlled Drug Delivery from Biotin-Doped Conductive Polypyrrole. *Adv. Mater.* **2006**, *18* (5), 577−581.

(21) Hamad-Schifferli, K.; Schwartz, J. J.; Santos, A. T.; Zhang, S.; Jacobson, J. M. Remote Electronic Control of DNA Hybridization through Inductive Coupling to an Attached Metal Nanocrystal Antenna. *Nature* **2002**, *415* (6868), 152−155.

(22) Thiesen, B.; Jordan, A. Clinical Applications of Magnetic Nanoparticles for Hyperthermia. *Int. J. Hyperthermia* **2008**, *24* (6), 467−474.

(23) Kim, Y.-J.; Ebara, M.; Aoyagi, T. A Smart Hyperthermia Nanofiber with Switchable Drug Release for Inducing Cancer Apoptosis. *Adv. Funct. Mater.* **2013**, *23* (46), 5753−5761.

(24) Cazares-Cortes, E.; Cabana, S.; Boitard, C.; Nehlig, E.; Griffete, N.; Fresnais, J.; Wilhelm, C.; Abou-Hassan, A.; Ménager, C. Recent Insights in Magnetic Hyperthermia: From the "Hot-Spot" Effect for Local Delivery to Combined Magneto-Photo-Thermia Using Magneto-Plasmonic Hybrids. *Adv. Drug Delivery Rev.* **2019**, *138*, 233−246.

(25) Mertz, D.; Sandre, O.; Bégin-Colin, S. Drug Releasing Nanoplatforms Activated by Alternating Magnetic Fields. *Biochim. Biophys. Acta, Gen. Subj.* **2017**, *1861* (6), 1617−1641.

(26) Norris, M. D.; Seidel, K.; Kirschning, A. Externally Induced Drug Release Systems with Magnetic Nanoparticle Carriers: An Emerging Field in Nanomedicine. *Adv. Ther.* **2019**, *2* (1), 1800092.

(27) Saint-Cricq, P.; Deshayes, S.; Zink, J. I.; Kasko, A. M. Magnetic Field Activated Drug Delivery Using Thermodegradable Azo-Functionalised PEG-Coated Core−Shell Mesoporous Silica Nanoparticles. *Nanoscale* **2015**, *7* (31), 13168−13172.

(28) Kong, S. D.; Zhang, W.; Lee, J. H.; Brammer, K.; Lal, R.; Karin, M.; Jin, S. Magnetically Vectored Nanocapsules for Tumor

Penetration and Remotely Switchable On-Demand Drug Release. *Nano Lett.* **2010**, *10* (12), 5088−5092.

(29) Mirvakili, S. M.; Hunter, I. W. Artificial Muscles: Mechanisms, Applications, and Challenges. *Adv. Mater.* **2018**, *30* (6), 1704407.

(30) Regmi, R.; Bhattarai, S. R.; Sudakar, C.; Wani, A. S.; Cunningham, R.; Vaishnava, P. P.; Naik, R.; Oupicky, D.; Lawes, G. Hyperthermia Controlled Rapid Drug Release from Thermosensitive Magnetic Microgels. *J. Mater. Chem.* **2010**, *20* (29), 6158−6163.

(31) Hu, S.-H.; Liu, T.-Y.; Liu, D.-M.; Chen, S.-Y. Controlled Pulsatile Drug Release from a Ferrogel by a High-Frequency Magnetic Field. *Macromolecules* **2007**, *40* (19), 6786−6788.

(32) Hoare, T.; Santamaria, J.; Goya, G. F.; Irusta, S.; Lin, D.; Lau, S.; Padera, R.; Langer, R.; Kohane, D. S. A Magnetically Triggered Composite Membrane for On-Demand Drug Delivery. *Nano Lett.* **2009**, *9* (10), 3651−3657.

(33) Uva, M.; Mencuccini, L.; Atrei, A.; Innocenti, C.; Fantechi, E.; Sangregorio, C.; Maglio, M.; Fini, M.; Barbucci, R. On the Mechanism of Drug Release from Polysaccharide Hydrogels Cross-Linked with Magnetite Nanoparticles by Applying Alternating Magnetic Fields: The Case of DOXO Delivery. *Gels* **2015**, *1* (1), 24−43.

(34) Shi, C.; Thum, C.; Zhang, Q.; Tu, W.; Pelaz, B.; Parak, W. J.; Zhang, Y.; Schneider, M. Inhibition of the Cancer-Associated TASK 3 Channels by Magnetically Induced Thermal Release of Tetrandrine from a Polymeric Drug Carrier. *J. Controlled Release* **2016**, *237*, 50−60.

(35) Ruggiero, M. R.; Geninatti Crich, S.; Sieni, E.; Sgarbossa, P.; Cavallari, E.; Stefania, R.; Dughiero, F.; Aime, S. Iron Oxide/PLGA Nanoparticles for Magnetically Controlled Drug Release. *Int. J. Appl. Electromagn. Mech.* **2017**, *53* (S1), S53−S60.

(36) Fang, K.; Song, L.; Gu, Z.; Yang, F.; Zhang, Y.; Gu, N. Magnetic Field Activated Drug Release System Based on Magnetic PLGA Microspheres for Chemo-Thermal Therapy. *Colloids Surf., B* **2015**, *136*, 712−720.

(37) Makadia, H. K.; Siegel, S. J. Poly Lactic-Co-Glycolic Acid (PLGA) as Biodegradable Controlled Drug Delivery Carrier. *Polymers* **2011**, *3* (3), 1377−1397.

(38) Das, P.; Colombo, M.; Prosperi, D. Recent Advances in Magnetic Fluid Hyperthermia for Cancer Therapy. *Colloids Surf., B* **2019**, *174*, 42−55.

(39) Mirvakili, S. M.; Sim, D.; Hunter, I. W.; Langer, R. Actuation of Untethered Pneumatic Artificial Muscles and Soft Robots Using Magnetically Induced Liquid-to-Gas Phase Transitions. *Sci. Robot.* **2020**, *5* (41), eaaz4239.

(40) Saris, N.-E. L.; Mervaala, E.; Karppanen, H.; Khawaja, J. A.; Lewenstam, A. Magnesium: An Update on Physiological, Clinical and Analytical Aspects. *Clin. Chim. Acta* **2000**, *294* (1), 1−26.

(41) Silva, V. A. J.; Andrade, P. L.; Silva, M. P. C.; Bustamante, D. A.; De Los Santos Valladares, L.; Albino Aguiar, J. Synthesis and Characterization of Fe3O4 Nanoparticles Coated with Fucan Polysaccharides. *J. Magn. Magn. Mater.* **2013**, *343*, 138−143.

(42) Grayson, A. C. R.; Choi, I. S.; Tyler, B. M.; Wang, P. P.; Brem, H.; Cima, M. J.; Langer, R. Multi-Pulse Drug Delivery from a Resorbable Polymeric Microchip Device. *Nat. Mater.* **2003**, *2* (11), 767−772.

(43) White, R. P.; Lipson, J. E. G. Polymer Free Volume and Its Connection to the Glass Transition. *Macromolecules* **2016**, *49* (11), 3987−4007.

(44) Shmool, T. A.; Zeitler, J. A. Insights into the Structural Dynamics of Poly Lactic-Co-Glycolic Acid at Terahertz Frequencies. *Polym. Chem.* **2019**, *10* (3), 351−361.

(45) Zolnik, B. S.; Leary, P. E.; Burgess, D. J. Elevated Temperature Accelerated Release Testing of PLGA Microspheres. *J. Controlled Release* **2006**, *112* (3), 293−300.

(46) Grayson, A. C. R.; Cima, M. J.; Langer, R. Size and Temperature Effects on Poly(Lactic-Co-Glycolic Acid) Degradation and Microreservoir Device Performance. *Biomaterials* **2005**, *26* (14), 2137−2145.

(47) Mirvakili, S. M.; Broderick, K.; Langer, R. S. A New Approach for Microfabrication of Printed Circuit Boards with Ultrafine Traces. *ACS Applied Materials & Interfaces* **2019**, *11* (38), 35376−35381.

(48) Sun, S.; Zeng, H.; Robinson, D. B.; Raoux, S.; Rice, P. M.; Wang, S. X.; Li, G. Monodisperse MFe2O4 (M = Fe, Co, Mn) Nanoparticles. *J. Am. Chem. Soc.* **2004**, *126* (1), 273−279.

■ NOTE ADDED AFTER ASAP PUBLICATION

This paper was published ASAP on June 9, 2020, with information missing from the Figure 2 caption. The corrected version was reposted on June 15, 2020.